Available online at www.sciencedirect.com
SCIENCE DIRECT®
Biosensors and Bioelectronics 20 (2005) 2131–2135
BIOSENSORS & BIOELECTRONICS
www.elsevier.com/locate/bios

Short communication

Frequency bandwidth limitation of external pulse electric fields in cylindrical micro-channel electrophoresis with analyte velocity modulation

Shau-Chun Wang[a,*], Hsiao-Ping Chen[a], Chia-Yu Lee[a], Leslie Y. Yeo[b]

[a] *Department of Chemistry and Biochemistry, 160 San-Hsing, Min-Hsiung, National Chung Cheng University, Chia Yi 621, Taiwan*
[b] *Department of Chemical and Biomolecular Engineering, University of Notre Dame, IN, USA*

Received 21 May 2004; received in revised form 5 August 2004; accepted 11 August 2004
Available online 27 September 2004

Abstract

In capillary electrophoresis, effective optical signal quality improvement is obtained when high frequency (>100 Hz) external pulse fields modulate analyte velocities with synchronous lock-in detection. However, the pulse frequency is constrained under a critical value corresponding to the time required for the bulk viscous flow, which arises due to viscous momentum diffusion from the electro-osmotic slip in the Debye layer, to reach steady-state. By solving the momentum diffusion equation for transient bulk flow in the micro-channel, we show that this set-in time to steady-state and hence, the upper limit for the pulse frequency is dependent on the characteristic diffusion length scale and therefore the channel geometry; for cylindrical capillaries, the set-in time is approximately one half of that for rectangular slot channels. From our estimation of the set-in time and hence the upper frequency modulation limit, we propose that the half width of planar channels does not exceed 100 μm and that the radii of cylindrical channels be limited to 140 μm such that there is a finite working bandwidth range above 100 Hz and below the upper limit in order for flicker noise to be effectively suppressed.
© 2004 Elsevier B.V. All rights reserved.

Keywords: Frequency modulation; Micro-channels; Electro-osmotic slip; Momentum diffusion.

1. Introduction

There are several advantages for using electrical fields with periodic waveforms in capillary and microchip electrophoretic separation. For example, biopolymer separation performance in gel electrophoresis and in micro-scale ratchet systems have been improved using pulse electric fields (Grossman, 1992; Slater et al., 1997).

External pulsed fields have also been used in analyte velocity modulation methods to enhance electrophoretic signal qualities via a synchronous demodulation detection scheme (Chen et al., 1989; Demana et al., 1992; Wang and Morris, 2000). The application of pulsed fields is particularly useful in suppressing optical interference arising from fluorescent microchip substrates. Lock-in detection is able to track a modulated electrophoretic signal regardless of background noise intensity, when fluorescence detection is used in plastic micro-channel devices. The spatial motion of analyte fluorophore is modulated with pulse fields when the analyte moves across the detection window while the motion of fluorophores on the plastic substrates remains stationary.

To obtain lower noise intensity, modulation frequencies have to be within the range in which thermal noise dominates since integration averaging effectively smoothes out the thermal noise. In contrast, flicker noise is not eliminated with ensemble average methods. Modulation frequencies below 100 Hz or less, where flicker noise is significant, therefore results in little signal quality improvement; modulation at higher frequencies provides more significant improvement.

* Corresponding author. Tel.: +886 5 2720411x66410; fax: +886 5 2721040.
E-mail address: chescw@ccu.edu.tw (S.-C. Wang).

0956-5663/$ – see front matter © 2004 Elsevier B.V. All rights reserved.
doi:10.1016/j.bios.2004.08.014

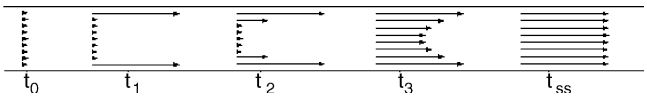

Fig. 1. Schematic illustration of the transient viscous flow velocity profiles from t_0, at which electric field is activated, to reach steady-state at t_{ss} where the velocity profile is flat indicating that the entire bulk flow is electro-osmotically driven.

The possible problem of differentiation resolution at the input end of lock-in amplifier hardware becomes secondary when a pre-amplifier is used to increase the signal by one or more orders of magnitude prior to feeding the signal into the lock-in circuit. Technically, the upper bound of modulation frequencies should therefore, be a minor concern.

Signal enhanced data reported elsewhere (Wang and Morris, 2000) contradicts the analysis that has been previously reported (Chen et al., 1989; Demana et al., 1992). The recovered signals via a lock-in amplifier were found to diminish as modulation frequencies increased beyond tens of cycles per second. We attribute this phenomenon to viscous diffusion limitations for momentum transfer from the electro-osmotically driven Debye layer into the bulk of the fluid (Wang, 2004). In such cases, the time required to reach steady-state after the external field is activated, known as the set-in time, becomes comparable to the duration over which momentum propagates over half the channel width. It is only when steady-state is achieved that the bulk of the fluid moves electro-osmotically with uniform speed through the micro-channel. The transient effects prior to steady-state are therefore attributed to viscous drag arising from electro-osmotic slip in the Debye layer. Fig. 1 schematically illustrates the transient evolution of viscous flow in a planar channel resulting in the final flat velocity profile at steady-state.

Transient effects of viscous flow due to electro-osmotic slip in the Debye layer in narrow capillaries have been studied (Tikhomolova, 1993). By simplifying the two-dimensional Navier–Stokes equation in the limit where the channel radius is sufficiently large compared to the Debye layer thickness such that the transient evolution of electro-osmotic flow within the Debye layer can be neglected, analytical solutions have been derived to describe the temporal variation of the viscous flow velocity at each point along the capillary radius at a given cross section (Wang, 2004). Similar approximation techniques have been employed in other studies (Ermakov et al., 1998; Patankar and Hu, 1998). These estimations have been found to agree with experimental data observed in micro-conduits of rectangular cross-section (Wang and Morris, 2000).

In this paper, we extend the simplified model described above to investigate the set-in time required to achieve steady-state bulk electro-osmotic flow in cylindrical geometries. In addition, scaling arguments are employed to estimate the set-in time for other asymmetrical channels typical of micro-conduits fabricated on microfluidic chips using solvent etching processes.

2. Theoretical model

2.1. Formulation

The flow of the electrolyte in the micro-channel can be described by the Navier–Stokes equation:

$$\rho\left(\frac{\partial \mathbf{u}}{\partial t} + \mathbf{u}\cdot\nabla\mathbf{u}\right) = -\nabla p + \mu\nabla^2\mathbf{u} + \rho_E\mathbf{E}, \tag{1}$$

where ρ is the fluid density, $\mathbf{u}$ the flow velocity, t the time, p the pressure between two ends of the micro-channel, μ the fluid viscosity, ρ_E the electrical polarization, and $\mathbf{E}$ the electrical field vector applied across the micro-channel. We consider an axisymmetric cylindrical conduit with radius R in a cylindrical coordinate system parameterized by z, r ($r \le R$), and, angle θ, respectively, as depicted in Fig. 2. The z-coordinate is aligned along the axis of the conduit perpendicular to the capillary cross-section.

Typically, the width of a rectangular slot or the diameter of a capillary representing the characteristic length scale of the micro-channel, approximately 100–200 μm, is much greater than the thickness of Debye layer for typical dilute electrolyte concentrations (1–10 mM), which is approximately 10–100 nm. Outside the Debye layer, the fluid can be assumed to be electroneutral. Since the channel width is much greater than the Debye layer thickness, it is possible to neglect the effects of the Debye layer and hence assume $\rho_E\mathbf{E} \sim 0$ in the bulk of the fluid. In addition, we also neglect the existence of any externally imposed pressure gradients across the channel ($\nabla p = 0$).

We now proceed to simplify (1) by adopting the following transformations:

$$u_z \to \frac{u_z}{U}, \quad u_r \to \frac{Lu_r}{RU}, \quad t \to \frac{Ut}{R}, \tag{2}$$

and

$$\lambda = \frac{r}{R}, \quad \zeta = \frac{z}{L}, \quad \tau = \frac{Ut}{R} = \frac{t}{(StR^2)}, \tag{3}$$

with

$$v_z = \frac{(U - u_z)}{U}, \tag{4}$$

where L is the length of the channel, U is the steady-state bulk electro-osmotic flow velocity governed by Helmholtz–Smoluchowski equation, and, St represents Stokes number

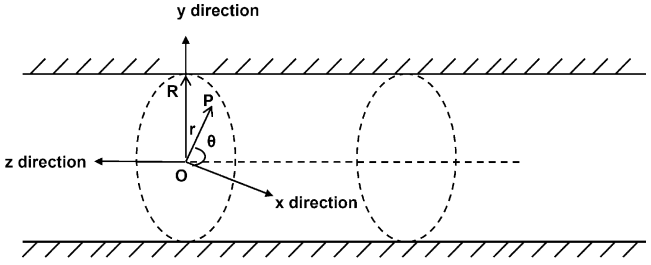

Fig. 2. The cylindrical coordinate system used.

ρ/μ. In the slender-body limit where $R \ll L$, it then follows that by employing the set of scalings given by (2) that (1) reduces to

$$\frac{\partial u_z}{\partial t} = \left(\frac{1}{St}\right)\left[\frac{1}{r}\frac{\partial}{\partial r}\left(r\frac{\partial u_z}{\partial r}\right)\right]. \tag{5}$$

Adopting the transformation in (3) and (4), we arrive at

$$\frac{\partial v_z}{\partial \tau} = \frac{1}{\lambda}\frac{\partial}{\partial \lambda}\left(\lambda\frac{\partial v_z}{\partial \lambda}\right), \tag{6}$$

where $0 \le v_z \le 1$, (6) is the usual diffusion equation that governs the transient dynamics of the viscous dominated flow in the bulk of the electrolyte arising due to electro-osmotic flow in the Debye layer.

2.2. Analytical solution

Given the initial condition $u_z = 0$ or $v_z = 1$ at $\tau = 0$, the symmetry boundary condition at $\lambda = 0$, which requires v_z to be bounded, and the no-slip boundary condition $v_z = 0$ at $\lambda = 1$, the solution of (6) has the form

$$v_z = \sum_{n=1}^{\infty} C_n \exp\left(-k_n \frac{St^{-1}}{R^2}t\right) J_0\left(\sqrt{k_n}\frac{r}{R}\right), \tag{7}$$

where $J_0\left(\sqrt{k_n}\lambda\right) = 1 + \sum_{n=1}^{\infty}\left[\left(\frac{(-1)^n k^n \lambda^{2n}}{2^{2n}(n!)^2}\right)\right]$ is the Bessel function of the first kind and

$$C_n = \frac{\int_0^R r J_0\left(\sqrt{k_n}\frac{r}{R}\right) \mathrm{d}r}{\int_0^R r {J_0}^2\left(\sqrt{k_n}\frac{r}{R}\right) \mathrm{d}r}. \tag{8}$$

We note that (7) is similar to the solution for the dimensionless temperature in the problem of a heated infinite solid cylinder in which the heat diffusion equation is solved. To leading order ($n = 1$),

$$v_z = 1.6 \exp\left(-5.78\frac{St^{-1}}{R^2}t\right) J_0\left(\sqrt{5.78}\frac{r}{R}\right). \tag{9}$$

At $r = 0$, $J_0(0) = 1$ and hence,

$$v_z(r = 0) = 1.6\exp(-5.78\tau). \tag{10}$$

At the center of the capillary $\lambda = 0$, we assume $u_z = 0.9U$ as the criterion for steady-state bulk electro-osmotic flow. It then follows from (4) that $v_z = 0.1$ when $u_z = 0.9U$. In (10), we note that $v_z = 0.1$ when $\tau = 0.480$ from which we deduce that t_{ss}, the set-in time to reach steady-state bulk electro-osmotic flow in the capillary, is therefore approximately $StR^2/2$. A similar solution to (7) was obtained for a rectangular slot using two-dimensional Cartesian coordinates (Wang, 2004):

$$v_x = \sum_{n=0}^{\infty} D_n \exp\left[-\left(n+\frac{1}{2}\right)^2 \pi^2 \frac{St^{-1}}{d^2}t\right] \times \cos\left(n+\frac{1}{2}\right)\left(\frac{\pi y}{d}\right), \tag{11}$$

where d is the channel half width and the coefficients D_n are defined by

$$D_n = \frac{2(-1)^n}{(n+1/2)\pi}. \tag{12}$$

For $v_x = 0.1$ at $y = 0$, we obtain the set-in time to reach steady-state bulk electro-osmotic flow in a rectangular slot $t_{ss} = 1.03Std^2$.

We now proceed to discuss briefly the accuracy of the leading order approximation. The squares of first five roots of $J_0\left(\sqrt{k_n}\right) = 0$ are as follows: 5.78, 30.5, 74.9, 139 and 223, which give the values for k_1, k_2, k_3, k_4 and k_5 in (7), respectively. Using (8), we obtain the following values for C_1, C_2, C_3, C_4, and C_5: 1.60, −1.26, −0.031, −0.00097 and −0.000074. At $r = 0$, the fifth order approximation of (7) is $v_z \sim \sum_{n=1}^{5} C_n \exp(-k_n\tau)$. For $\tau = 0.5$, we find that, with the exception of the first term which has a value of about 0.09, the next four higher order terms all have values less than 10^{-6} and hence have negligible contribution to the sum. It is therefore, possible to conclude that the first order approximation used previously is sufficiently accurate to estimate the set-in time to achieve steady-state bulk electro-osmotic flow. Similarly, from (11) at $y = 0$ and $\tau = 1$ whilst the first term has a value of approximately 0.10, the next four higher order terms carry values which are less than 10^{-19} and hence it is possible to obtain an accurate estimate of v_x to leading order.

2.3. Estimation of the set-in time to achieve steady-state bulk electro-osmotic flow

The movement of weakly adsorbed ions within the Debye layer provides momentum that drags the bulk fluid in the channel in order to generate the viscous flow. This momentum is created at the edges in the Debye layer and propagates toward the center of the channel over a characteristic time for viscous diffusion that is inversely proportional to the fluid viscosity. For highly viscous fluids, the momentum transfer is therefore large giving rise to a shorter characteristic time. In other words, the momentum diffusion is faster in more viscous media. In addition, since momentum is proportional to liquid density, the diffusion speed is slower for more dense fluids.

We estimate that it takes tens to hundreds of milliseconds ($\sim\rho R^2/\mu$) to achieve steady-state bulk electro-osmotic flow in sub-millimeter channels or capillaries. When a periodic waveform is used to generate modulated electro-osmotic drag viscous flows, the waveform period should therefore be longer than this characteristic time scale so that the momentum created in the Debye layer has sufficient enough time to propagate to the center of the channel. In comparing the experimental data reported previously with our theoretical analysis, it is possible to conclude that analyte velocity in micro-channels therefore cannot be modulated at frequencies beyond the critical value predicted by our theoretical analysis.

From (7) and (11), it is possible to estimate the time required to achieve steady-state bulk electro-osmotic flow t_{ss} in a cylindrical capillary as well as that for a rectangular slot channel:

$$t_{ss} = 0.48\frac{\rho R^2}{\mu}, \quad (13)$$

for cylindrical capillaries, and

$$t_{ss} = 1.03\frac{\rho d^2}{\mu}, \quad (14)$$

for rectangular slots. We therefore note that t_{ss} for a cylindrical channel is one-half of that for the rectangular slot channel.

3. Results and discussion

3.1. Typical set-in times and upper modulation frequency limits

From (14), we estimate the upper limit for the modulation frequency $\mu/(\rho d^2)$ to be approximately 100 Hz for a rectangular slot channel with half width 100 μm fabricated on plastic substrates. Given that aqueous solutions are most commonly used in micro-fluidic applications, we typically assume the fluid medium of water with density ρ = 1 g/cm^3 and viscosity μ = 0.01 dyne s/cm^2 is assumed as the fluid medium (Wang, 2004). Clearly, this upper limit is close to the lower frequency limit of approximately 100 Hz required to suppress significant flicker noise. This agrees with the narrow working bandwidth range for the modulation frequency in experiments where relatively large rectangular channels with half widths above 100 μm have been employed. If the channel half width were to be reduced by half to 50 μm, the upper limit increases to 400 Hz, therefore indicating the strong dependence of the channel dimensions on the working bandwidth range and suggesting the advantage of using smaller channels. This will be discussed further below.

Capillary electrophoresis, on the other hand, employs cylindrical conduits with internal diameters, which are less than 100 μm. From (13), we estimate the upper limit for the frequency to be approximately 800 Hz for a 50 μm channel radius. However, as modulation frequencies above 500 Hz have not been used (Chen et al., 1989; Demana et al., 1992), frequency dependence on the demodulated signal intensities has, therefore not been observed, as expected. The observation of frequency dependence would be anticipated if an upper frequency limit lower than 500 Hz is predicted, as would be the case if (14) for rectangular geometries were to be wrongly extrapolated to cylindrical geometries. The prior discussion therefore suggests the importance of channel dimensions and geometry on the frequency bandwidth limitations and provides a reasonable explanation for the experimental observations.

3.2. Extension to asymmetrical channel geometries

Similar to mass diffusion, momentum diffusion in viscous media is isotropic. Since, there is no orientation preference, viscous diffusivity increases with the degrees of freedom for momentum propagation. In our analysis, the magnitude of viscous diffusion is approximately twice in two-dimensional geometries to that for one-dimensional channels. This two-fold enhancement should be valid for all two-dimensional cases. In all micro-channels fabricated on chip substrates, both symmetrical and asymmetrical, momentum propagation has two degrees of freedom. It thus follows that the steady-state electro-osmotic set-in time $t_{ss} = 0.5\,\rho l^2/\mu$, where l is the characteristic length of the channel, is approximately equal to that in (13). The argument above agrees with the estimation of the characteristic frequency in a two-dimensional mixing chamber driven by electrokinetics at moderate field strengths of 100 V/cm (Sundaram and Tafti, 2004).

3.3. Maximum suggested channel dimensions to suppress flicker noise

In order to maintain a finite modulation frequency bandwidth for flicker noise suppression, the upper frequency modulation limit, constrained by a set-in time, which characterizes the diffusion limitation within the system, must exceed the lower frequency limit of 100 Hz, below which flicker noise is significant. Since, the set-in time scales as the square of the characteristic channel length scale l, there is a critical maximum channel dimension such that the upper frequency limit is above 100 Hz. In other words, the channel dimension has to be sufficiently small such that set-in time does not exceed 0.01 s. Assuming water as the working fluid, which is typical of the aqueous solutions commonly used, we estimate that the half width of planar channels should not exceed 100 μm whereas the radii of cylindrical capillaries should be limited to 140 μm, in order for flicker noise suppression by analyte velocity modulation to be effective.

Acknowledgements

The authors acknowledge the financial support provided by the National Science Council, Taiwan (NSC 92-2113-M-194-022) and the National Chung Cheng University.

References

Chen, C.-Y., Demana, T., Huang, S.D., Morris, M.D., 1989. Capillary zone electrophoresis with analyte velocity modulation. Application to refractive index detection. Anal. Chem. 61 (14), 1590–1593.

Demana, T., Guhathakurata, U., Morris, M.D., 1992. Effects of analyte velocity modulation on the electroosmotic flow in capillary electrophoresis. Anal. Chem. 64 (4), 390–394.

Ermakov, S.V., Jacobson, S.C., Ramsey, J.M., 1998. Computer simulations of electrokinetic transport in microfabricated channel structures. Anal. Chem. 70 (21), 4494–4504.

Grossman, P.D., 1992. Capillary Electrophoresis: Theory and Practice. Academic Press, San Diego.

Patankar, N.A., Hu, H.H., 1998. Numerical simulation of electroosmotic flow. Anal. Chem. 70 (9), 1870–1881.

Slater, G.W., Guo, H.L., Nixon, G.I., 1997. Bidirectional transport of polyelectrolytes using self-modulating entropic ratchets. Phys. Rev. Lett. 78 (6), 1170–1173.

Sundaram, N., Tafti, D.K., 2004. Evaluation of microchamber geometries and surface conditions for electrokinetic driven mixing. Anal. Chem. 76 (13), 3785–3793.

Tikhomolova, K.P., 1993. Electro-osmosis. Harwood, New York.

Wang, S.-C., 2004. Frequency bandwidth limitation of external pulse electric field in microchannels. Applications to analyte velocity modulation detections. Biosens. Bioelectron. 20 (1), 139–142.

Wang, S.-C., Morris, M.D., 2000. Plastic microchip electrophoresis with analyte velocity modulation. Application to fluorescence background rejection. Anal. Chem. 72 (7), 1448–1452.